

# Thermodynamics of rotating black hole in the presence of cold dark matter

Swapan Kumar Majhi

*Ranaghat College, Nadia, West Bengal-741201, India*

E-mail: majhi.majhi@gmail.com

## Abstract

We have computed the thermodynamic properties of a rotating black holes in the presence of cold dark matter. The dependence of temperaure, Gibbs free energy, specific heat on the horizon radius have been studied for various values of critical density ( $\rho_c$ ) of the cold dark matter. The studies shows that only small values of critical density of cold the dark matter, black hole are stable.

# 1 Introduction

In recent years, the study of dark matter(DM) is an emerging area of research which basically connects cosmology and particle physics [1, 2]. Current observations indicate that DM is nearly invisible and hence can not be directly observed but its existence can be observed through indirect evidence [3], for example microwave background radiation measurements [4] weak gravitational lensing effects [5, 6], measurements of galaxy rotation [7, 8, 9], large scale structure measurements [10, 11], galaxy light-to-mass ratios [12] and cluster dynamics measurements [13, 14]. Among various dark matter models, the cold dark matter(CDM) model is one of the predominant models for dark matter [15, 16]. It is composed of neutral weakly interacting heavy particles [17] and the number of DM is very large [18]. Vera Rubin's [7] observations of the motion of stars within galaxies is one of the prime evidence in early 1980s and it predicted more concentrated matter distribution in the galaxies than predicted by gravitational effects which points the strong support for the theory of dark matter. The Wilkinson Microwave Anisotropy Probe (WMAP) produced the first image of the infant universe and accurately measured the cosmological parameters in 2003. The same result obtained by the Sloan Digital Sky Survey (SDSS) which confirm the existence of dark matter [19]. The rapid development of gravitational wave astronomy[20, 21, 22, 23, 24, 25] and the successful capture of black hole images in 2019[26, 27, 28], black holes have become another favourite topic of research area among physicists. It has been noticed [29, 30, 31, 32] that there exist supermassive black holes along with the dark matter particles in the central regions of galaxies. Both black hole and dark matter can form stable system in the central region of galaxies[32]. The detailed study of their interactions and dynamics will reveal the nature of dark matter as well as black holes.

One of the interesting feature of black hole physics is their thermodynamic properties. The pioneer works of Hawking and Bekenstien [33]-[35] opened up the new direction in this context. First time, they have pointed out that there is an interesting resemblance between the spacetimes with horizons and the thermodynamical systems with well defined temperature and entropy. In these works, they have showed that the black hole behaves like a thermal systems and laws of black hole mechanics are basically same as laws of thermodynamics. Very first time, Hawking *et. al.* [33]-[35] tried to construct entropy of the black hole event horizon using phenomenological models. Black hole entropy and thermodynamic properties have been studied extensively various cases like Schwarzschild space time [33]-[37], Reissner-Nordstrom black hole [38] and rotating and non-rotating black hole [39]-[46]. The study of thermodynamic properties of black hole has revealed many aspects of their physics and hence it is very important to investigate the black holes presence of dark matter and and their thermodynamical properties.

In this article, we begin with a short review of spacetime metric in section 2. In section 3, we have calculate various thermodynamic variables like Bekenstein-Hawking entropy, Hawking temperature, Gibbs free energy and specific heat etc. with numerical plots and their discussions. At the end, we summarise. We have used units which fix the speed of light and gravitational constant  $G = C = 1$  and also used the scale radius  $R_s = 1$  for simplicity, through out our numerical analysis.

## 2 Space-time metric of rotating black hole in the presence of Dark Matter

The distribution of dark matter halos within galaxies can be described using several parameters, including scale radius and critical density, which emerge from the interactions among dark matter particles. When a black hole resides at the geometric center of a dark matter halo, there can be series of interactions between the black hole and the encompassing dark matter halo. The dark matter-black hole systems can be precisely characterized by employing the steady-state approximate black hole metric. In this work, we consider the cold dark matter halos as determined by the cold dark matter model.

According to Navarro-Frenk-White (NFW) profile, the density distribution of the dark matter halo

in the cold dark model is given by [15, 48, 49]

$$\rho_{NFW} = \frac{\rho_c}{\frac{r}{R_s} \left(1 + \frac{r}{R_s}\right)^2} \quad (1)$$

where  $\rho_c$  denotes the critical density of the dark matter halo and  $R_s$  represents the scale radius of the dark matter halo. In a dark matter halo scenario, the spacetime metric of a rotating black hole [47] is

$$\begin{aligned} ds^2 = & - \left[ 1 - \frac{r^2 + 2Mr - r^2 \left(1 + \frac{r}{R_s}\right)^{-\frac{8\pi\rho_c R_s^3}{r}}}{\Sigma^2} \right] dt^2 \\ & + \frac{2a \sin^2 \theta}{\Sigma^2} \left[ r^2 + 2Mr - r^2 \left(1 + \frac{r}{R_s}\right)^{-\frac{8\pi\rho_c R_s^3}{r}} \right] dt d\phi \\ & + \frac{\sin^2 \theta}{\Sigma^2} \left[ (r^2 + a^2)^2 - \Delta a^2 \sin^2 \theta \right] d\phi^2 + \frac{\Sigma^2}{\Delta} dr^2 + \Sigma^2 d\theta^2 \end{aligned} \quad (2)$$

with

$$\Sigma^2(r, \theta) = r^2 + a^2 \cos^2 \theta \quad (3)$$

$$\Delta(r) = a^2 - 2Mr + r^2 \left(1 + \frac{r}{R_s}\right)^{-\frac{8\pi\rho_c R_s^3}{r}} \quad (4)$$

where  $M$  is the black hole mass,  $a$  is rotational parameter. As the dark matter critical density ( $\rho_c$ ) goes to zero, the above metric reduces to *Kerr's* rotational black hole metric.

We have calculated the scalar invariants like Ricci scalar and Kretschmann scalar. The Ricci scalar is proportional to  $\Sigma^{-2}$  and has a simple form

$$R = \frac{-2 + \partial_r^2 \Delta(r)}{\Sigma^2(r, \theta)} \quad (5)$$

whereas the Kretschmann scalar  $R_{\mu\nu\rho\sigma} R^{\mu\nu\rho\sigma}$  is proportional to  $\Sigma^{-6}$  i.e.

$$R_{\mu\nu\rho\sigma} R^{\mu\nu\rho\sigma} = \frac{f(r, a, \theta)}{\Sigma^6(r, \theta)}. \quad (6)$$

The function  $f(r, a, \theta)$  is regular as  $\theta = \frac{\pi}{2}$  and  $r \rightarrow 0$  and too large to reproduce here. At  $\theta = \frac{\pi}{2}$  and  $r \rightarrow 0$ , metric eqn.(2) possesses a singularity called ring singularity which also presents in Ricci scalar and Kretschmann scalar.

From the Einstein tensor, we have calculated the density and pressure of the energy momentum tensor of rotating dark matter case as given below:

$$\begin{aligned} \rho &= -P_r = -\frac{(a^2 - r^2 - \Delta(r) + r\partial_r \Delta(r))}{\Sigma(r, \theta)^4} \\ P_\theta &= P_\phi = -\frac{(a^2(1 + \cos^2 \theta) - \Delta(r) + r\partial_r \Delta(r))}{\Sigma(r, \theta)^4} + \frac{\partial_r^2 \Delta(r)}{2\Sigma(r, \theta)^2} \\ &= -P_r + \frac{1}{2\Sigma(r, \theta)^2} (\partial_r^2 \Delta(r) - 2) \end{aligned} \quad (7)$$

It is clear from the above expression eqn.(7) that the physical ring singularity is also present in the energy density and the pressure. In the right panel of the figure 1, we have plotted  $P_\theta$  and  $\rho + P_\theta$  and showed that both are positive outside the horizon.

## 2.1 Event horizon and Ergosphere

Here we will discuss briefly the horizons and ergosphere region of the rotating black hole surrounded by the cold dark matter. They play crucial role (specially event horizon ( $r_h^+$ )) to find the thermodynamic variables of the black hole.

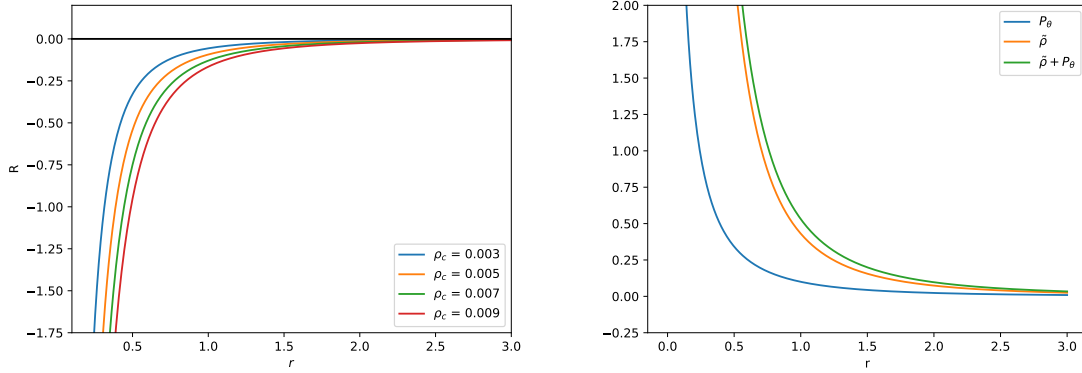


Figure 1: Left panel is the variation of Ricci scalar with respect to the radial coordinate  $r$  with various values of dark matter critical densities  $\rho_c$  and other parameters considered to be one. Right panel represents the variation of Einstein's energy density and pressure.

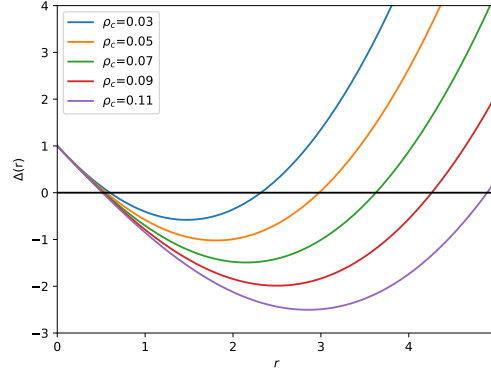


Figure 2: Variation of  $\Delta(r)$  with respect to radial coordinate  $r$  with various dark matter density.

The condition to find the event horizon radius is  $g^{rr} = 0$  which gives

$$\Delta(r) = 0. \quad (8)$$

Event horizon radius can be calculated from the eqn.(4) as given below

$$a^2 - 2Mr + r^2 \left(1 + \frac{r}{R_s}\right)^{-\frac{8\pi\rho_c R_s^3}{r}} = 0. \quad (9)$$

The exact analytical solution of eqn.(9) can not be found but one can solve numerically. However the horizon radius can be put in the simple form as given below

$$r_h = M \pm M \sqrt{1 - \frac{a^2 - r_h^2 + r_h^2 \left(1 + \frac{r_h}{R_s}\right)^{-\frac{8\pi\rho_c R_s^3}{r_h}}}{M^2}} \quad (10)$$

In the figure(2), we have plotted the  $\Delta(r)$  with respect to radial coordinate  $r$  with various values of critical densities of cold dark matter and showed that there are two horizons one is called inner horizon ( $r_h^-$  cauchy horizon) and other one is called outer horizon ( $r_h^+$ , event horizon). In this figure, the points where change in sign indicate the horizon radius. Both the horizon depend nontrivially on the dark

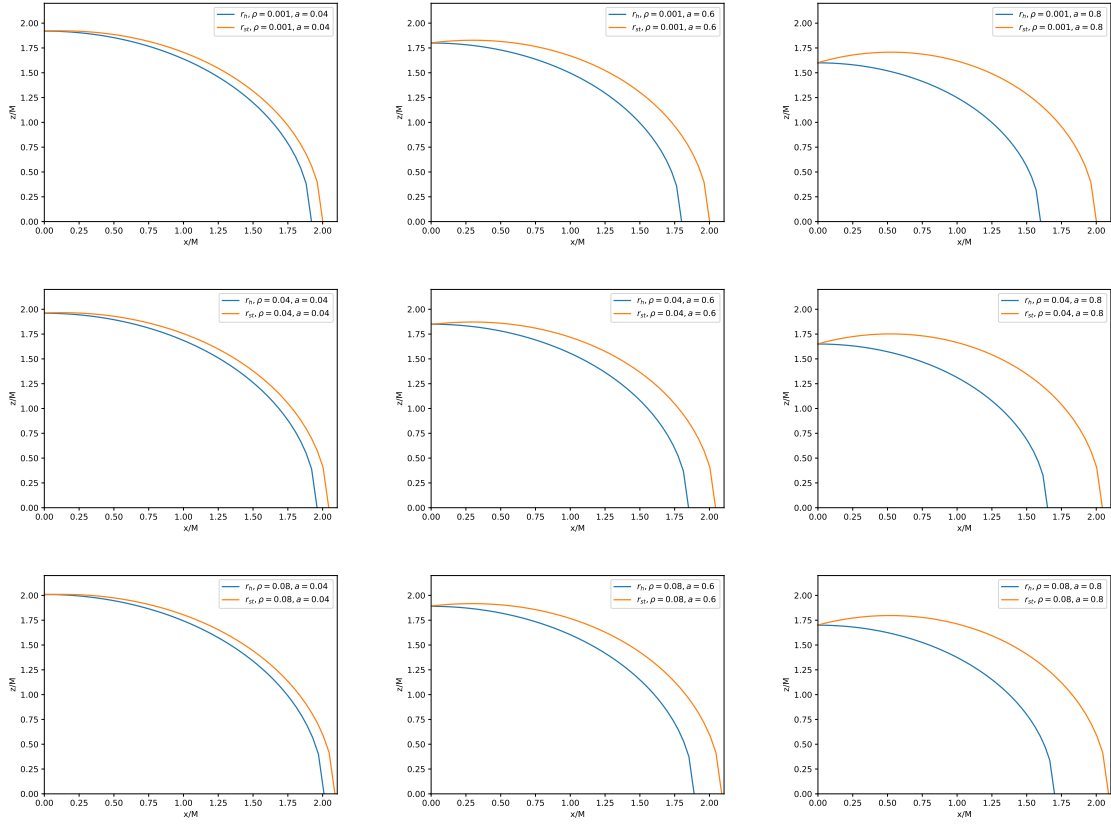


Figure 3: Behavior of ergoregion in the  $xz$  plan with different values of critical densities

matter parameter ( $\rho_c$ ). Horizon radii increase with increase of critical density ( $\rho_c$ ) as shown in the figure 2.

Ergosphere is a region between the event horizon and static limit surface. The static limit surface is defined by  $g_{tt} = 0$  i.e.

$$\Delta(r) - a^2 \sin^2 \theta = 0. \quad (11)$$

Similar to the event horizon solution, static limit surface has two solutions ( $r_{sls}^-, r_{sls}^+$ ). The region between the event horizon ( $r_h^+$ ) and positive root of static limit surface ( $r_{sls}^+$ ) is the ergosphere region. Comparing eqns(9,11), we find that both horizon radius and static limit radius coincide each other at  $\theta = 0$  or  $\pi$ . In the figure 3, we have plotted event horizon and ergosphere in the  $x$ - $z$  plane with various values of rotational parameter  $a$  and critical density of cold dark matter. At the equatorial plane ( $\theta = \pi/2$ ), static radius does not depend on the rotational parameter  $a$ . As we increase the value of rotation parameter  $a$ , the horizon radius ( $r_h$ ) decreases hence the region of ergospace increases.

### 3 Thermodynamics of rotating black hole in the presence of Dark Matter

In the section, we have discussed the thermodynamical properties of rotating black hole in the presence of cold dark matter. We have computed all the thermodynamics variables like Bekenstein-Hawking entropy, Hawking's temperature, Gibb's free enegy and Specific heat at the event horizon ( $\Delta(r) = 0$ ).

For the given metric in eqn.(2), the Bekenstein-Hawking entropy of the black hole can be calculated

from the area of the horizon as

$$S_{BH} = \frac{1}{4G_N} \int d\theta d\phi \sqrt{g_{\theta\theta}g_{\phi\phi}} = \frac{1}{4G_N} \int d\theta d\phi \sin\theta \sqrt{(r^2 + a^2)^2 - \Delta a^2 \sin^2\theta} \quad (12)$$

At the horizon  $\Delta(r_h) = 0$ , after integration one can get the simple form as given below

$$S_{BH} = \frac{\pi(r_h^2 + a^2)}{G_N} \quad (13)$$

From the above eqn(13), it apparently seems that the Bekenstein-Hawking entropy  $S_{BH}$  does not depend on the any of the dark matter halo parameters like dark matter critical density,  $\rho_c$  or scale radius of the dark matter halo  $R_s$  explicitly. However, it does depend on the these parameters through horizon radius.

Now we want to calculate the hawking temperature of the rotating black hole in the presence of cold dark matter. The hawking temperature of the rotating black hole can be calculated various methods like by computing the surface gravity [39, 40] or by the standard Euclidean procedure [52, 53]. In this article, we have follow the the standard Euclidean procedure. For completeness, we have briefly reviewed the procedure. We defined two orthogonal killing vectors

$$\begin{aligned} \xi &= \partial_t + \frac{a}{a^2 + r^2} \partial_\phi, & \tilde{\xi} &= a \sin^2\theta \partial_t + \partial_\phi \\ \xi^2 &= -\frac{\Delta \Sigma^2}{(a^2 + r^2)^2}, & \tilde{\xi}^2 &= \Sigma^2 \sin^2\theta, & \xi \cdot \tilde{\xi} &= 0 \end{aligned} \quad (14)$$

The vectors  $\xi$  and  $\tilde{\xi}$  are the dual to each other and null on the horizon i.e.  $\xi^2(r_h) = 0$ ,  $\tilde{\xi}^2(r_h) = 0$ . It is assume that  $\xi$  is time-like everywhere outside the horizon  $r \geq r_h$ , whereas the vector  $\tilde{\xi}$  is space-like everywhere outside the axis ( $\theta = 0$ ,  $\theta = \pi$ ) where  $\tilde{\xi}^2 = 0$ . The 1-form corresponding to  $\xi$  and  $\tilde{\xi}$  are

$$d\omega = \frac{a^2 + r^2}{\Sigma^2} (dt - a \sin^2\theta d\phi), \quad d\tilde{\omega} = \frac{a^2 + r^2}{\Sigma^2} \left(-\frac{a}{a^2 + r^2} dt + d\phi\right) \quad (15)$$

With standard Euclideanization of time variable  $t = i\tau$  and along with the transformation of the rotating parameter  $a = i\hat{a}$ , the Euclidean killing vectors  $\xi, \tilde{\xi}$  and their dual 1-form  $d\omega, d\tilde{\omega}$  take form

$$\begin{aligned} \xi &= \partial_\tau + \frac{\hat{a}}{\hat{a}^2 + r^2} \partial_\phi, & \tilde{\xi} &= \hat{a} \sin^2\theta \partial_\tau + \partial_\phi \\ d\omega &= \frac{r^2 - \hat{a}^2}{\hat{\Sigma}^2} (d\tau - \hat{a} \sin^2\theta d\phi), & d\tilde{\omega} &= \frac{r^2 - \hat{a}^2}{\hat{\Sigma}^2} \left(\frac{\hat{a}}{r^2 - \hat{a}^2} d\tau + d\phi\right) \end{aligned} \quad (16)$$

where  $\hat{\Sigma}^2 = r^2 - \hat{a}^2 \cos^2\theta$ . The Euclidean metric reduces to

$$ds_E^2 = -\frac{\hat{\Delta} \hat{\Sigma}^2}{(r^2 - \hat{a}^2)^2} d\omega^2 - \frac{\hat{\Sigma}^2}{\hat{\Delta}} dr^2 - \hat{\Sigma}^2 (d\theta^2 + \sin^2\theta d\tilde{\omega}^2) \quad (17)$$

with  $\hat{\Delta} = -\hat{a}^2 - 2Mr + r^2 \left(1 + \frac{r}{R_s}\right)^{-\frac{8\pi\rho_c R_s^3}{r}}$  which will give the horizon radius  $r = r_h^+$  ( $\hat{r}_h$ ). Introducing new radial coordinate  $x$  near the horizon

$$\begin{aligned} \hat{\Delta} &= \gamma(r - \hat{r}_h) = \frac{\gamma^2 x^2}{4} \\ \gamma &= (\hat{r}_h - r_-) \end{aligned} \quad (18)$$

the Euclidean metric near horizon becomes

$$ds_E^2 = -\hat{\Sigma}_h^2 \left(dx^2 + \frac{\gamma^2 x^2}{4(\hat{r}_h^2 - \hat{a}^2)^2} d\omega^2\right) - \hat{\Sigma}_h^2 (d\theta^2 + \sin^2\theta d\tilde{\omega}^2) \quad (19)$$

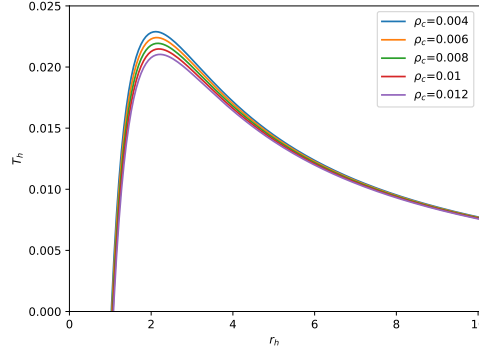


Figure 4: variation of Hawking temperature ( $T_h$ ) with respect to horizon radius with various values of cold dark matter critical density ( $\rho_c$ ).

On the horizon surface  $\mathcal{H}$ , introducing a new coordinate  $\psi = \phi + \frac{\hat{a}\tau}{\hat{r}_h^2 - \hat{a}^2}$ , the surface horizon metric can be written as

$$ds_{\mathcal{H}}^2 = \hat{\Sigma}_h^2(d\theta^2 + \sin^2\theta d\tilde{\omega}^2) = \hat{\Sigma}_h^2(d\theta^2 + \frac{(\hat{r}_h - \hat{a}^2)^2}{\hat{\Sigma}_h^4} \sin^2\theta d\psi) \quad (20)$$

The points  $\psi$  and  $\psi + 2\pi$  should be identified on the horizon  $\mathcal{H}$  for the regularity of the metric at points  $\theta = 0$  and  $\theta = \pi$ . The full metric now turns into

$$ds_E^2 = -\hat{\Sigma}_h^2 ds_{C_2}^2 - ds_{\mathcal{H}}^2 \quad (21)$$

where  $ds_{C_2}^2$  is the metric on the two dimensional disk  $C_2$  given by

$$ds_{C_2}^2 = dx^2 + \frac{\gamma^2 x^2}{4(\hat{r}_h^2 - \hat{a}^2)^2} d\omega^2 \quad (22)$$

By introducing a new angle coordinate  $\chi = \tau - \hat{a} \sin^2\theta \phi$  the metric on the disk can be put in the following form

$$ds_{C_2}^2 = dx^2 + \frac{\gamma^2 x^2}{4\hat{\Sigma}_h^4} d\chi^2 = dx^2 + x^2 d\left(\frac{\gamma}{2\hat{\Sigma}_h^2} \chi\right)^2 \quad (23)$$

This metric is very similar form as plane polar coordinate if the angle variable,  $\frac{\gamma}{2\hat{\Sigma}_h^2}$  has the period of  $2\pi$  and has a conical singularity at  $x = 0$ . To avoid this conical singularity one needs to identify the points  $\chi$  and  $\chi + 4\pi\hat{\Sigma}_h^2\gamma^{-1}$ . This turns out to be the points  $(\tau, \phi)$  and  $(\tau - \beta_h, \phi - \Omega_h \beta_h)$  must be identified on the horizon  $\mathcal{H}$ , where  $\beta_h = 4\pi\hat{\Sigma}_h^2\gamma^{-1}$  is the inverse Hawking temperature of the black hole and  $\Omega = \hat{a}/(\hat{r}_h^2 - \hat{a}^2)$  is the angular velocity. By analytically continued to the real values  $a$ , the Hawking temperature of rotating black hole with cold dark matter is given as

$$T_h = \frac{1}{\beta_h} = \frac{1}{4\pi} \frac{\gamma}{r_h^2 + a^2} \quad (24)$$

where

$$\gamma = \frac{1}{r_h} \left[ \left(1 + r_h/R_s\right)^{\frac{-8\pi\rho_c R_s^3}{r_h}} \left( r_h^2 + 8\pi\rho_c R_s^3 \left( r_h \ln(1 + r_h/R_s) - \frac{r_h^2}{r_h + R_s} \right) \right) - a^2 \right] \quad (25)$$

In figure 4, we have plotted Hawking temperature with respect to horizon radius for various values of critical density of CDM. There are two black hole branches at a given temperature. The first branch, where the temperature increases with radius, is stable and occurs for small values of  $r_h$ . Conversely, the second branch, where the temperature decreases with radius, is unstable and occurs for large  $r_h$ .

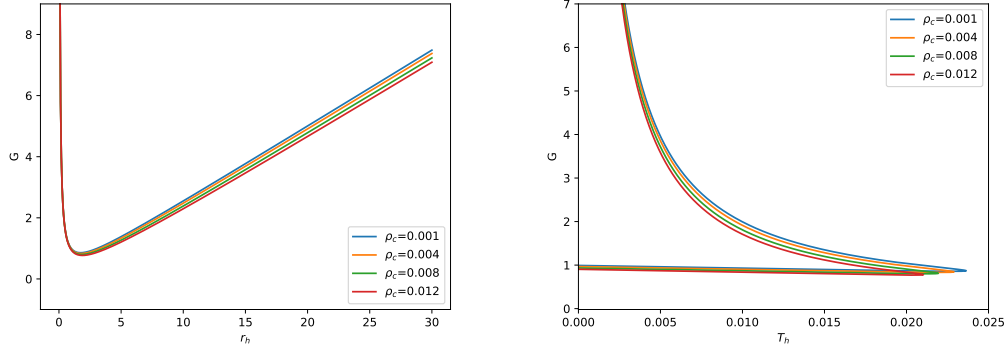


Figure 5: Left panel is the variation of Gibb's free energy ( $\mathcal{G}$ ) with respect to horizon radius with variour values of cold dark matter critical density ( $\rho_c$ ) and right panel represents the variation of Gibb's free energy ( $\mathcal{G}$ ) with respect to Hawking temperature ( $T_h$ ).

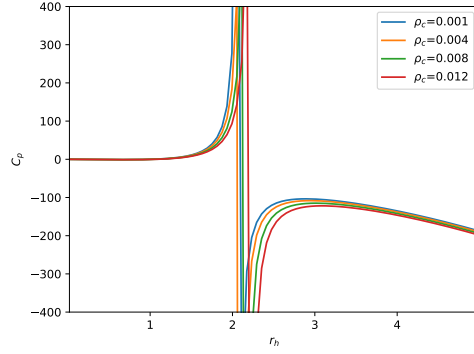


Figure 6: Variation of specific heat ( $C_p$ ) with respect to horizon radius ( $r_h$ ).

The thermodynamic stability or instability of these small and large black hole branches will be further confirmed through an analysis of free energy and specific heat.

The Gibbs free energy is given by[41, 42]:

$$\mathcal{G} = \mathcal{M} - T_h S_{BH} \quad (26)$$

In figure(5), we have plotted Gibb's free energy ( $\mathcal{G}$ ) with respect to the Hawking temperature ( $T_h$ ) with different values of critical densities ( $\rho_c$ ) of cold dark matter. In this figure, the horizon radius  $r_h$  increases from left to right. For a fixed temperature, there are two black hole branches. The lower branch corresponds to more stable black hole with smaller Gibb's free energy and positive specific heat ( $C_p > 0$ ). Whereas the upper branch corresponds to unstable black hole (Schwarzschild-like black hole) with higher free energy and negative specific heat ( $C_p < 0$ ).

In figure(6), we have plotted specific heat ( $C_p = T_h(\partial S_{BH}/\partial T_h)$ ) with respect to the horizon radius with various values of critical densities ( $\rho_c$ ) of cold dark matter. From this figure we notice that specific heat is positive for small black hole branch and negative for large black hole branch as we have stated earlier. So positivity of specific heat in small black hole branch shows thermodynamically stable in nature whereas negativity of specific heat in large black hole branch implies the thermodynamically stable in nature.

## 4 Conclusions

In this article, we have computed geometrical quantities like Ricci scalar Kretschmann scalar, Einstein energy momentum tensor of a rotating black hole in the presence of cold dark matter and showed that it is very similar to the *Kerr's* rotating black hole in the critical limit ( $\rho_c \rightarrow 0$ ). We have studied the effect of cold dark matter critical density on event horizons and ergosphere region. We find that by increasing the critical density, increases the border of both the horizons and ergosphere for a fixed value of rotational parameter  $a$ . It is also noticed that for a fixed value of critical density ( $\rho_c$ ), the horizon radius decreases with increasing the rotational parameter  $a$  and hence the area between the horizon and static limit surface increases.

We also studied the thermodynamic stability of rotating black hole with cold dark matter scenario. The qualitative features remain same as *Kerr's* case but quantitatively found corrections due to cold dark matter presence. Specifically, we observe thermodynamically stable small black hole branches alongside unstable large ones similar to the *Kerr's* case. This feature is clearly visible in all the thermodynamical variables, noticeably in Gibb's free energy ( $\mathcal{G}$ ) and Specific heat ( $C_p$ ). We have also discovered that the stability of the rotating black hole in the presence of cold dark matter, within certain horizon radius and temperature ranges, is intricately influenced by the parameter critical density.

There are numerous intriguing avenues to explore further in this study. It would be interesting to study the dynamical stability of these black holes against various perturbations. Another intriguing area to explore involves investigating thermal fluctuations, by incorporating the system's corrected entropy using partition function[54, 55, 56]. It would be compelling to examine how the presence of the cold dark matter impacts various phenomena such as the black hole shadow, gravitational waves, photon orbits, quasi-normal modes, and Hawking radiation, and to discern these effects from those observed in the Kerr case. We are considering these issues for our future investigation.

## Acknowledgements

We would like to thank Dr. Anindya Biswas for useful discussion. SM would like to thank the Department of Physical Sciences, IISER Kolkata for hospitality while part of the project was being carried out. SM also acknowledges the Science and Engineering research Board, India for financial assistance under the Teachers Associateship for Research Excellence (TARE) grant.

## References

- [1] X. Bi, Y. Fan, Q. Yue, Y. Zhou, What is dark matter? Chinese Sci. Bull. 63, 2413–2421 (2018)
- [2] Y. Zhou, Progress in the study of dark matter properties and detection of dark matter (in Chinese). Sci. China Phys. Mech. Astron.58(2), 020421 (2015)
- [3] J.H. Oort, The force exerted by the stellar system in the direction perpendicular to the galactic plane and some related problems. Bull.Astron. Inst. Neth. 6, 249 (1932)
- [4] Z. Shen, K. Duan, Z. Xu et al., The fire-eye and dark matter line spectrum search of the “wukong” satellite. Chin. Sci. Bull. 67(13),1421–1422 (2022)
- [5] J. Zhang, A precise measurement method for weak gravitational lensing effect, in Proceedings of the 2014 Galaxy Cosmology Frontiers Workshop of the Chinese Astronomical Society, Shanghai Jiao Tong University, Yangzhou, pp. 1–45 (2014)
- [6] N.N. Weinberg, M. Kamionkowski, Weak gravitational lensing by dark clusters. Mon. Not. R. Astron. Soc. 337(4), 1269–1281 (2002)

- [7] V.C. Rubin, N. Thonnard, W.K. Jr. Ford, Rotational properties of 21 SC galaxies with a large range of luminosities and radii, from NGC 4605  $R = 4$  kpc to UGC 2885  $R = 122$  kpc. *ApJ* 238(2), 471–471 (1980)
- [8] Ekaterina V. Karukes, Paolo Salucci, The universal rotation curve of dwarf disc galaxies. *Mon. Not. R. Astron. Soc.* 465, 4703–4722 (2016)
- [9] M.S. Roberts, A.H. Rots, Comparison of rotation curves of different galaxy types. *Astron. Astrophys.* 26(3), 483–485 (1973)
- [10] L. Fang, S. Xiang, S. Li, Dark matter in the universe and the formation of large-scale structure: dark matter components and clustering scenario. *Sci. China (Ser. A: Math. Phys. Astron. Technol. Sci.)* 27(9), 832–840 (1984)
- [11] L. Gao, Large-scale structures in the universe. *Sci. Obs.* 15(1), 33–36 (2020)
- [12] Z. Zhong, G. Zhao, Research progress on the mass-to-light ratio of different celestial bodies. *Prog. Astron.* 36(2), 81–100 (2018)
- [13] T.A. Tagliaferro, A. Biviano, G. De Lucia, E. Munari, D.G. Lambas, Dynamical analysis of clusters of galaxies from cosmological simulations. *Astron. Astrophys.* 652, A90 (2021)
- [14] F. Zwicky, Die Rotverschiebung von extragalaktischen Nebeln. *Helv. Phys. Acta* 6, 110–127 (1933)
- [15] Navarro, J. F., Frenk, C. S., White, S. D. M. 1996. The Structure of Cold Dark Matter Halos. *The Astrophysical Journal* 462, 563. doi:10.1086/177173
- [16] Navarro, J. F., Frenk, C. S., White, S. D. M. 1997. A Universal Density Profile from Hierarchical Clustering. *The Astrophysical Journal* 490, 493508. doi:10.1086/304888
- [17] X. Bi, B. Qin, Dark matter and dark matter particle detection. *Physics* 40(01), 13–17 (2011)
- [18] P.A.R. Ade, N. Aghanim, M.I.R. Alves, C. Armitage-Caplan, M. Arnaud, M. Ashdown, F. Atrio-Barandela, J. Aumont, H. Aussel, C. Baccigalupi, A.J. Banday, R.B. Barreiro, R. Barrena, M. Bartelmann, J.G. Bartlett, N. Bartolo, S. Basak, E. Battaner, R. Battye, K. Benabed et al., Planck 2013 results. I. Overview of products and scientific results. *Astron. Astrophys.* 571, A1 (2014)
- [19] C. Seife, Illuminating the dark universe. *Science* 302(5653), 2038–2039 (2003)
- [20] Y. Hu, J. Mei, J. Luo, Tianqin project and international collaboration. *Chin. Sci. Bull.* 64(24), 2475–2483 (2019)
- [21] Z. Zhu, Y. Wang, Prediction, detection, and discovery of gravitational waves. *Physics* 45(05), 300–310 (2016)
- [22] J. Liu, G. Wang, Y. Hu et al., First detection event GW150914 of gravitational waves and gravitational wave astronomy. *Chin. Sci. Bull.* 61(14), 1502–1524 (2016)
- [23] B.P. Abbott et al., Observation of gravitational waves from a binary black hole merger. *Phys. Rev. Lett.* 116(6), 061102 (2016)
- [24] B.P. Abbott et al., Gw170817: observation of gravitational waves from a binary neutron star inspiral. *Phys. Rev. Lett.* 119(16), 161101 (2017)
- [25] B.P. Abbott et al., GWTC-1: a gravitational-wave transient catalog of compact binary mergers observed by LIGO and Virgo during the first and second observing runs. *Phys. Rev. X* 9(3), 031040 (2019)
- [26] K. Akiyama et al., First M87 event horizon telescope results. I. The shadow of the supermassive black hole. *Astrophys. J. Lett.* 875, L1 (2019)
- [27] K. Akiyama et al., First M87 event horizon telescope results. VI. The shadow and mass of the central black hole. *Astrophys. J. Lett.* 875(1), L6 (2019)

- [28] K. Akiyama et al., First M87 event horizon telescope results. V. Physical origin of the asymmetric ring. *Astrophys. J. Lett.* 875(1), L5 (2019)
- [29] D. Lynden-Bell, Galactic nuclei as collapsed old quasars. *Nature* 223, 690–694 (1969)
- [30] A. Eckart, R. Genzel, Stellar proper motions in the central 0.1 pc of the galaxy. *Mon. Not. R. Astron. Soc.* 284(3), 576–598 (1997)
- [31] K. Gebhardt, J. Adams, D. Richstone, T.R. Lauer, S.M. Faber, K. Gültekin, J. Murphy, S. Tremaine, The black hole mass in M87 from Gemini/NIFS adaptive optics observations. *Astrophys. J.* 729(2), 119 (2011)
- [32] J. Kormendy, D.O. Richstone, Inward bound—the search for super-massive black holes in galactic nuclei. *Annu. Rev. Astron. Astro-phys.* 33, 581–624 (1995)
- [33] J. D. Bekenstein, *Phys. Rev.* **D7** (1973) 2333  
*Phys. Rev.* **D9** (1974) 3292
- [34] S.W. Hawking, *Nature (London)* **248**: (1974) 30  
*Commun. Math. Phys* 43:(1975)199  
*Commun. Math. Phys* 25:(1972)152
- [35] J. M. Bardeen, B. Carter, and S. W. Hawking,, *Commun. Math. Phys* 31:(1973)161
- [36] S.W. Hawking, *Commun. Math. Phys* 46:(1976)206
- [37] R.M. Wald, *Living Rev.Relativ.* 4 (2001) 6, arXiv:gr-qc/9912119.
- [38] M.R.R. Good and Y.C. Ong, *Eur.Phys.J. C* **80** (2020) 1169
- [39] A. Fatima, K. Saifullah, *Astrophys. Space Sci.* 361 (2016) 161.
- [40] S.H. Hendi, S. Hajkhalili, M. Jamil M. Momennia, *Eur.Phys.J. C* **81** (2021) 1112.
- [41] S. Mahapatra, I. Banerjee, *Phys. Dark Universe* 39 (2023) 101172, arXiv:2208.05796[gr-qc].
- [42] D.V. Singh, S. Upadhyay, M.S. Ali, *Int. J. Mod. Phys.A* **37**(2022)2250049, arXiv:2206.05057[gr-qc].
- [43] A. Ditta, X. Tiecheng, G. Mustafa, M. Yasir, F. Atamurotov, *Eur.Phys.J. C* **82** (2022) 756
- [44] M. Yasir, X. Tiecheng, A. Ditta, F. Atamurotov, *New Astron.* 105 (2024) 102106.
- [45] A. Ditta, X. Tiecheng, R.Ali, F. Atamurotov, A. Mahmood, S. Mumtaz, *Ann. Phys.* 453 (2023) 169326.
- [46] F. Javed, A. Basit, A. Caliskan, E. Gudekli, *Frontiers in Astronomy and Space Sciences* 10,1174029.
- [47] Xu, Z., Hou, X.,Gong, X., Wang, J. 2018. Black hole space-time in dark matter halo. *Journal of Cosmology and Astroparticle Physics* 2018. doi:10.1088/1475-7516/2018/09/038;
- [48] Dubinski, J., Carlberg, R. G. 1991. The Structure of Cold Dark Matter Halos. *The Astrophysical Journal* 378, 496. doi:10.1086/170451
- [49] R. A. Konoplya and A. Zhidenko, Solutions of the Einstein Equations for a Black Hole Surrounded by a Galactic Halo, *Astrophys.J.* 933 (2022) 2, 166.
- [50] Ureña-López, L. A., Matos, T., Becerril, R. 2002. Inside oscillatons. *Classical and Quantum Gravity* 19, 62596277. doi:10.1088/0264-9381/19/23/320
- [51] Harko, T. 2011. Bose-Einstein condensation of dark matter solves the core/cusp problem. *Journal of Cosmology and Astroparticle Physics* 2011. doi:10.1088/1475-7516/2011/05/022
- [52] G. W. Gibbons and S. W. Hawking, “Action Integrals and Partition Functions in Quantum Gravity,” *Phys. Rev.* **DD15** (1977) 2752D 15 (1977) 2752–2756.

- [53] R. B. Mann and S. N. Solodukhin, “Conical geometry and quantum entropy of a charged Kerr black hole,” *Phys. Rev.***DD 54** (1996) 3932 (1996) 3932–3940, arXiv:hep-th/9604118.
- [54] M. Sharif, G. Abbas, *Chin. Phys. Lett.* 29 (2012) 010401, arXiv:1202.1705[physics.gen-ph]
- [55] B. Pourhassan, K. Kakobi, Z. Sabery. *Ann.Phys.* 399 (2018) 181. arXiv: 1811.03152 [gr-qc]
- [56] S. Gunasekaran, D. Kabiznak, R.B. Mann, *J. High Energy Phys.* 2012 (2012) 1.